Methodology for thermal design of novel combined refrigeration/power binary fluid systems

Na Zhang[a,*], Noam Lior[b]

[a]*Institute of Engineering Thermophysics, Chinese Academy of Sciences, Beijing 100080, P. R. China*
[b]*Department of Mechanical Engineering and Applied Mechanics, University of Pennsylvania, Philadelphia, PA 19104-6315, USA*

Abstract

Refrigeration cogeneration systems which generate power alongside with cooling improve energy utilization significantly, because such systems offer a more reasonable arrangement of energy and exergy "flows" within the system, which results in lower fuel consumption as compared to the separate generation of power and cooling or heating. This paper proposes several novel systems of that type, based on ammonia–water working fluid. Importantly, general principles for integration of refrigeration and power systems to produce better energy and exergy efficiencies are summarized, based primarily on the reduction of exergy destruction. The proposed plants analyzed here operate in a fully-integrated combined cycle mode with ammonia–water Rankine cycle(s) and an ammonia refrigeration cycle, interconnected by absorption, separation and heat transfer processes. It was found that the cogeneration systems have good performance, with energy and exergy efficiencies of ∼28% and 55–60%, respectively, for the base-case studied (at maximum heat input temperature of 450 °C). That efficiency is, by itself, excellent for cogeneration cycles using heat sources at these temperatures, with the exergy efficiency comparable to that of nuclear power plants. When using exhaust heat from topping gas turbine power plants, the total plant energy efficiency can rise to the remarkable value of about 57%. The hardware proposed for use is conventional and commercially available; no hardware additional to that needed in conventional power and absorption cycles is needed.
© 2007 Elsevier Ltd and IIR. All rights reserved.

Keywords: Cogeneration; Design; Absorption system; Ammonia–water

Méthodologie pour la conception thermique de systèmes de cogénération (production de froid et d'énergie) utilisant des fluides binaires

Mots clés : Cogénération ; Conception ; Système à absorption ; Ammoniac–eau

* Corresponding author. Tel.: +86 10 82543030; fax: +86 10 62575913.
E-mail address: zhangna@mail.etp.ac.cn (N. Zhang).

Nomenclature

E	exergy (kW)		ΔT_P	pinch point temperature difference (K)
h	specific enthalpy (kJ/kg)		η_1	energy efficiency (%)
m	mass flow rate (kg/s)		η_2	exergy efficiency (%)
p	pressure (kPa)		*Subscripts*	
p_b	turbine back-pressure (kPa)		a	ambient state
Q	heat duty (kW)		EVA	evaporator
R	refrigeration/power ratio		hs	heat source fluid
RR	Rectifier molar reflux ratio		in	input
SF	Split fraction		i	inlet
s	specific entropy (kJ/kg K)		REB	reboiler
T	temperature (K)		REC	rectifier
t	temperature (°C)		T	turbine
W	power output (kW)		1, 2, …, 29	states on the cycle flow sheet
X	ammonia mass fraction			

1. Introduction

Refrigeration cogeneration systems which generate power alongside with cooling improve energy utilization significantly, because such systems offer a more reasonable arrangement of energy and exergy ''flows'' within the system, which results in lower fuel consumption as compared to the separate generation of power and cooling or heating [1]. This is a practical way to improve overall system efficiency when both refrigeration and power are needed. Goswami et al. [2] proposed a combined power/refrigeration cycle using mixed working fluids and investigated its performance [3–8]. In their system, the ammonia-rich vapor from a rectifier unit, which is about 20% of the total mass flow, first expands in a turbine to generate power and then the cold turbine exhaust provides cooling by transferring only sensible heat to the chilled water. The amount of produced cooling is relatively small, and none would be produced for high turbine inlet temperature; hence the system was mainly intended to be operated with low temperature heat sources including geothermal or solar.

One of the ways that such cogeneration systems can have improved performance is by reducing the exergy loss in the heat transfer process from a variable temperature heat source, by concurrently varying the temperature of the heat sink and thus making the temperature difference between the heat source and sink more uniform along the heat exchanger (cf. [9]). This can be accomplished in a number of ways, one, most suitable when absorption refrigeration is used, is using binary-component working fluids that exhibit a variable boiling temperature during the boiling process. The ammonia–water mixture is one of the most widely used working fluids in refrigeration machines. Maloney and Robertson [10] proposed the use of an ammonia–water mixture as the working fluid in an absorption power cycle. In the combined power cycle proposed by Kalina [11], an ammonia–water mixture was employed as the working fluid

in the bottoming cycle. A comparison conducted by Ibrahim and Klein [12] concluded that the Kalina cycle produces under certain conditions more power than the Maloney and Robertson cycle. These systems have power as their only usable output. Even the insertion of the absorption refrigeration unit in Wang et al.'s work [13] was not for the generation of cooling, but just to help increase the power output. Integration of the refrigeration and power components driven by the same external heat source can be accomplished by a number of configurations, several of which are proposed, analyzed and compared in this paper. An attempt is also made here to develop and demonstrate a basic general methodology for the favorable integration of such systems.

2. The main principles for system integration

The fact that refrigeration and power cycles generally operate in different temperature regions can be used in a synergistic way. For example, power cycles have some middle/low temperature heat outputs, which are impractical for generating additional power because of their low temperatures, but might be a suitable heat source for an absorption refrigeration cycle. Similarly, in the cooling cycles, some cooling capacity may exist that is not cold enough for refrigeration, but could be an appropriate heat sink to the power cycle. Their intelligent integration thus has the potential for creating a new combined cycle or cogeneration system that may have a higher efficiency.

In the cogeneration systems proposed in this paper, there are two fully-integrated sub-cycles: an absorption refrigeration cycle and a Rankine power cycle, interconnected by the absorption, separation, and heat transfer processes. They use the same working fluid, a mixture of ammonia and water, but with different concentrations, and they are supplied with heat by one external heating fluid. The energy input to the system is via several heat

exchangers, and to obtain high efficiency they should be arranged in a cascade according to their temperature level. Within each heat exchanger, small temperature differences should be maintained to allow for a good thermal match between the hot and cold streams.

Binary-component mixtures exhibit a boiling temperature that varies during the boiling process (as the concentration of the low-bubble-temperature substance keeps decreasing in the liquid phase), and their employment as working fluids thus allows maintenance of a more constant temperature difference between them and variable temperature heat sources, and consequently reduces exergy losses in the heat addition process. To have an increasing temperature during the evaporation process, the working fluid concentration should be neither too high nor too low, to be able to produce the necessary temperature glide.

Condensation of the binary working fluid is a temperature varying process too. To attain complete condensation, the fluid bubble point temperature should be higher than the cooling water inlet temperature by at least the minimal heat transfer temperature difference that allows use of practical heat exchanger sizes. Since ammonia has a lower saturation temperature than water for a given pressure, completing the condensation of ammonia–water mixtures at the same temperature results in a higher pressure than that for pure water. A binary working fluid in the power turbine thus expands to a higher back-pressure, which is an advantage in that it prevents air leakage into the system, but is unfavorable for power generation. In the Kalina cycle, this problem is addressed by an absorption–condensation process, in which a weaker stream from the bottom of the flash tank dilutes the turbine exhaust so that the latter can be condensed at a lower pressure [11]. Some other ways to address this problem were investigated in Refs. [13,14].

For better efficiency, the physical exergy of any pressure differences in the system, needed for the process, should also be recovered properly, and here we replace the conventional absorption refrigeration weak solution throttling device, which simply destroys the pressure difference exergy, by a power generating turbine.

3. The performance criteria and main assumptions used

Despite many attempts, the method for properly quantifying disparate outputs, such as power, heating, and refrigeration produced by the same system, to the overall performance, still remains unclear (cf. [8,15]). In this paper, the most commonly used energy efficiency and exergy efficiency definitions are adopted for the system performance evaluation.

The analyzed systems have two useful outputs: refrigeration and power. The cycle can be heated by the flue gas of a gas turbine or any other heat source of suitable temperature, entering at the hot end of the boiler. In this paper, the heat source fluid is chosen to be air (79% N_2 and 21% O_2 by volume).

Since the heating fluid is finally exhausted to the environment, the calculation of the efficiencies is based on its initial state. The energy efficiency is the ratio between the total useful energy outputs to the heat input from the heating fluid:

$$\eta_1 = (Q_{\text{EVA}} + W)/Q_{\text{in}} \tag{1}$$

where

$$Q_{\text{in}} = m_{\text{hs}}(h_{\text{hs,i}} - h_{\text{hs,a}}) \tag{2}$$

and where W is the power output from the turbine, reduced by the power input to the pumps, and $h_{\text{hs,i}}$ is the initial enthalpy of the heating fluid entering the system.

Since the energy efficiency weighs the refrigeration and power outputs, as well as the heat input, equally, even though the quality of these energies is rather different, exergy efficiency is a more proper evaluation criterion in this case, and in the evaluation of cogeneration systems with more than one kind of energy output or input in general.

The exergy efficiency is defined as the exergy output divided by the exergy input to the cycle:

$$\eta_2 = (E_{\text{EVA}} + W)/E_{\text{in}} \tag{3}$$

where the exergy of the heating fluid, E_{in}, is defined as:

$$E_{\text{in}} = m_{\text{hs}}\left[(h_{\text{hs,i}} - h_{\text{hs,a}}) - T_{\text{a}}(s_{\text{hs,i}} - s_{\text{hs,a}})\right] \tag{4}$$

$h_{\text{hs,a}}$ and $s_{\text{hs,a}}$ are the enthalpy and entropy, respectively, of the heat source fluid at ambient temperature and pressure.

The exergy of refrigeration, E_{EVA}, is calculated as the working fluid exergy difference across the evaporator EVA, because the chilled fluid in the EVA is undefined.

It is assumed that the system operates at steady state. The simulations were carried out using the commercial Aspen Plus [16] code, in which the component models are based on energy, mass and species balances, with the default relative convergence error tolerance of 0.01%; the thermal properties were calculated with the thermal property method of the Electrolyte NRTL model or the SR-Polar model for high temperatures (>246 °C) and pressures (>100 bar) applications. To validate the properties calculations, the property results from Aspen Plus and the data published by the International Institute of Refrigeration [17] were compared, and the result shows good agreement between them. For example, the absolute error of the water mass percentage in saturated NH_3/H_2O vapor is within 1%, and increases to 3–4% only in the high pressure region (>5 MPa). The average relative error of boiling point temperature is ~2.6%. The main assumptions for the calculations are summarized in Table 1.

The proposed cogeneration systems could be used as a bottom cycle in a combined cycle system, with a gas turbine as the topping cycle. Since the flue gas temperature of common gas turbines of small size or middle size is about 500 °C, the binary turbine inlet temperature is

Table 1
Main assumptions for the base-case calculation

Cycle parameter	
Cooling water temperature t_w (°C)	30.0
Evaporator EVA	
Pressure p_{EVA} (kPa)	160
Pressure loss (%)	3.0
Outlet temperature (°C)	−15
(High pressure) Absorber $ABS_{(H)}$	
Absorption pressure (kPa)	155
Pressure loss (%)	3.0
Outflow vapor fraction	0
Ambient state	
Temperature t_a (°C)	25.0
Pressure p_a (kPa)	101.3
Turbine T	
Inlet temperature (°C)	450.0
Isentropic efficiency (%)	87
Rectifier REC	
Theoretical stage number	6
Molar reflux ratio RR	0.3
Operation pressure p_{REC} (kPa)	1400
Pressure loss (%)	3.0
Feed stream vapor fraction	0
Reboiler REB	
Outlet temperature t_{REB} (°C)	165
Heat exchangers (B, REB, HEX, CON, C, ABS)	
Pinch point temperature difference ΔT_P (K)	5 or 15 (if one side is air)
Pressure loss (%)	1.0−3.0
Pumps P	
Efficiency (%)	75
Heat source	
Fluid	Air (79% N_2, 21% O_2)

chosen to be 450 °C in this study, because ammonia starts dissociating at higher temperatures to nitrogen and hydrogen, although some past studies (cf. [11]) have assumed its use in power cycles up to 532 °C. In the condensers CON and the absorbers ABS, the working fluid is cooled by 30 °C water. This relatively high cooling water temperature was chosen to produce reasonably conservative performance results.

Three cogeneration cycle configurations are studied below.

4. The parallel refrigeration/power combined cycle

This plant combines an ammonia refrigeration cycle and an ammonia−water Rankine cycle in parallel, as shown in Fig. 1. The power cycle can be identified as 6−7−8−9−10−11−1 and the refrigeration cycle as 14−15−16−17−18−1. They connect together in the process 1−2−3−4/12−···−6/14. Correspondingly, the working fluid has three primary concentration levels: the basic concentration solution in the process 1−2−3; the weak concentration solution in the power cycle 6−7−8−9−10−11, and the high concentration solution in the refrigeration cycle 14−15−16−17−18. The combined cycle also has four pressure levels: high (7−8) and low (9−10) in the power cycle, and two intermediate ones in the rectification process (2−3−4/12−···−6/14−15) and the refrigeration (16−17−18) and absorption processes (18/11−1).

One important motivation in the development of this cycle was the recognition that proper operation of the absorption cooling cycle requires the generator to be at a significantly higher pressure than the absorber (here the pressure ratio is ∼9), and that the weak solution flow (which is about 80% of total work fluid mass flow rate) from the generator to the absorber is just throttled for creating this pressure drop. Such throttling is rather wasteful, and a calculation for a simple conventional ammonia−water absorption refrigeration system (not cogeneration), with the main parameters the same as those in Table 1, has shown that its exergy efficiency is merely about 15% when heated by the heating fluid with the same temperature. Introduction of a steam-driven power generation system in lieu of the throttling valve, with heat addition to vaporize the weak solution, allows generation of power alongside with refrigeration produced by the absorption system.

The calculations are based on a unit mass flow rate (1.0 kg/s) of the basic working fluid fed to the rectifier. Table 2 summarizes the parameters, including temperature t, pressure p, vapor fraction, mass flow rate m and ammonia mass fraction X, of each stream of the cycle flow sheet.

The system performances are reported in Table 3; good performance is obtained, with the energy efficiency and exergy efficiency being 28 and 56%, respectively. The exergy efficiency is much higher than the energy efficiency because the external heat source fluid is at a relatively low temperature and its exergy content is hence much lower than its energy content.

Fig. 2 is the $t−Q$ diagram of the cycle heat addition process. The heat duty Q is normalized by the cycle energy input Q_{in} (Eq. (2)), to show more clearly the fraction of heating fluid energy utilized in the system. To get a better temperature match with the heat source fluid, the positions of the boiler B, the reboiler REB, and the heat exchanger HEX, are arranged (cascaded) in the plant according to their temperature levels.

An exergy analysis is performed to decompose the exergy losses in the different subsystems and sub-processes, as shown in Fig. 3. It can be seen that the two biggest losses occur in the heat addition (B, REB and HEX) and condensation processes, thus identifying these processes as having the greatest potential for exergy use improvement. They are followed by the turbine, where the losses can be reduced by using a more efficient turbine. The exergy loss in the refrigeration production process (EVA, C and V) is the smallest, in large part because of the way it is calculated here, based on the working fluid side, without considering the heat transfer exergy destruction with the undefined cooled medium.
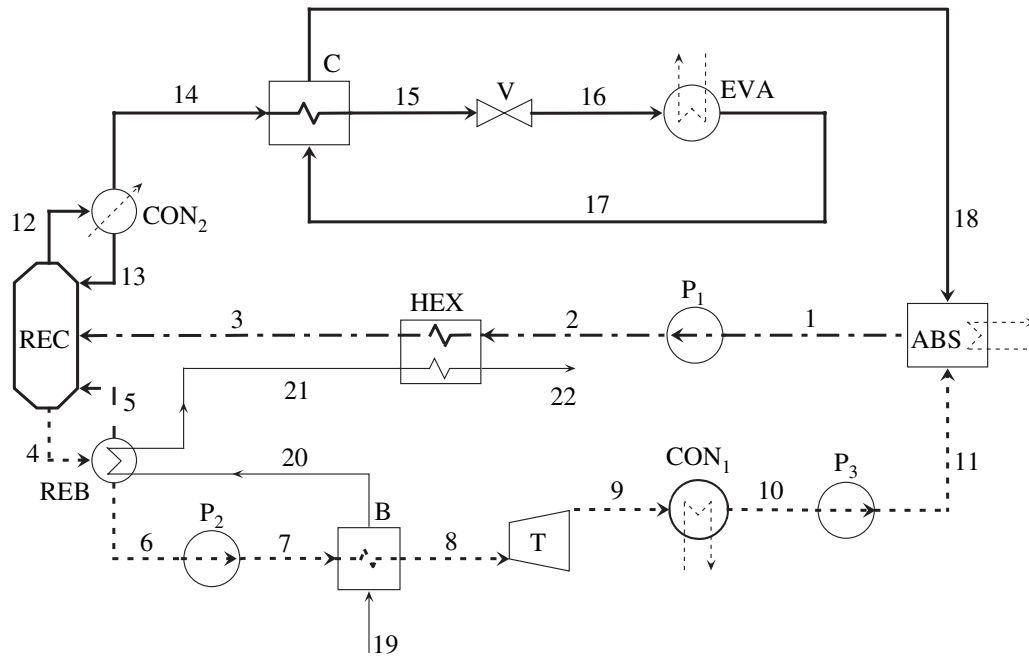
Fig. 1. The flow sheet of the parallel power/refrigeration cycle. ABS, absorber; B, boiler; C, cooler; CON, condenser; EVA, evaporator; HEX, heat exchanger; P, pump; REB, reboiler; REC, rectifier; T, turbine; V, valve. (—·—·—) basic concentration; (————) heat source fluid; (············) cooling water; (————) high concentration (refrigeration sub-cycle); (·······) low concentration (power sub-cycle).

Table 2
The refrigeration/power parallel cogeneration cycle stream states (the state numbers refer to Fig. 1)

State no.	t (°C)	p (kPa)	Vapor fraction	h (kJ/kg)	s (kJ/kg K)	m (kg/s)	X
Working fluid							
1	40.4	150	0	−12,494.4	−9.775	1	0.3
2	40.7	1484	0	−12,492.2	−9.771	1	0.3
3	117.9	1442	0	−12,030.1	−8.535	1	0.3
4	134.5	1400	0	−12,760.6	−7.905	1.09	0.221
5	165	1400	1	−7564.46	−4.385	0.317	0.522
6	165	1400	0	−14,131.9	−7.537	0.771	0.098
7	166.2	5253	0	−14,124.6	−7.531	0.771	0.098
8	450	5100	1	−11,597.6	−2.762	0.771	0.098
9	56.7	19.1	0.908	−12,541	−2.335	0.771	0.098
10	35	18.6	0	−14,789.8	−9.248	0.771	0.098
11	35	155	0	−14,789.6	−9.248	0.771	0.098
12	88.2	1400	1	−2805.46	−6.628	0.298	0.979
13	37.5	1400	0	−4082.64	−10.696	0.069	0.979
14	37.5	1400	0	−4082.64	−10.696	0.229	0.979
15	−9.2	1358	0	−4341.3	−11.562	0.229	0.979
16	−22.7	165	0.051	−4341.3	−11.524	0.229	0.979
17	−15	160	0.9	−3181.27	−6.893	0.229	0.979
18	32.5	155	0.99	−2922.6	−5.947	0.229	0.979

No.	t (°C)	p (kPa)	Vapor fraction	h (kJ/kg)	s (kJ/kg K)	m (kg/s)	Mole composition	
							N_2	O_2
Heat source fluid								
19	465	104.3	1	459.725	1.081	7.6	0.79	0.21
20	224.2	103.3	1	203.546	0.665	7.6	0.79	0.21
21	149.5	102.3	1	126.525	0.5	7.6	0.79	0.21
22	89.9	101.3	1	65.725	0.348	7.6	0.79	0.21

Table 3
Performance summary for the parallel cogeneration system

Turbine T work (kW)	726.9
Pump work (kW)	
P_1	2.2
P_2	5.6
P_3	0.15
Refrigeration output Q_{EVA} (kW)	266.2
Condenser CON_1 load (kW)	1732.7
Rectifier condenser CON_2 load (kW)	381.0
Cooler C load (kW)	59.4
Absorber ABS heat load (kW)	427.9
Boiler B heat input (kW)	1947.1
Reboiler REB heat input (kW)	585.4
Heat exchanger HEX heat input (kW)	462.1
Net power output W (kW)	719.0
Refrigeration/power ratio R	0.37
Heat input Q_{in} (kW)	3496.0
Exergy input E_{in} (kW)	1379.6
Energy efficiency η_1 (%)	28.2
Exergy efficiency η_2 (%)	55.8

In this cycle, the working fluid in the power sub-cycle is a weak solution from the reboiler; its physical exergy of pressure is recovered for power generation. The working fluid has a low ammonia concentration (0.098) in both the heat addition and condensation processes; this has both advantages and disadvantages. The power turbine has a relatively low back-pressure, but the temperature in the evaporation process does not change very much, leading to a poor match with the heating fluid variable temperature in the evaporation process. This is consistent with the exergy analysis results showing that the exergy loss in the heat
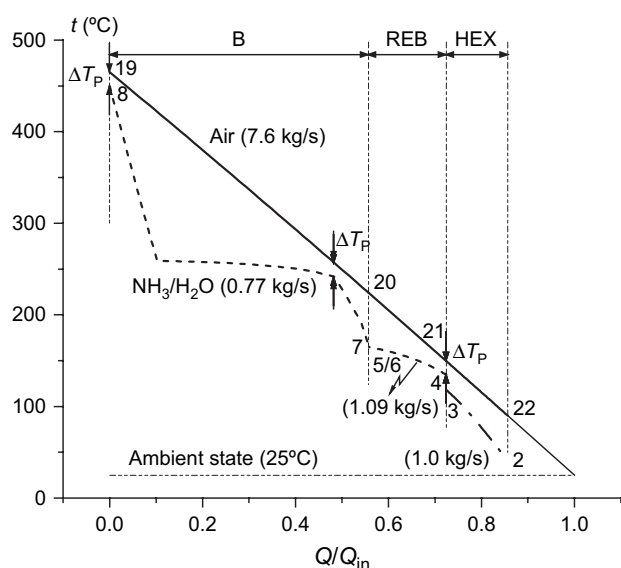

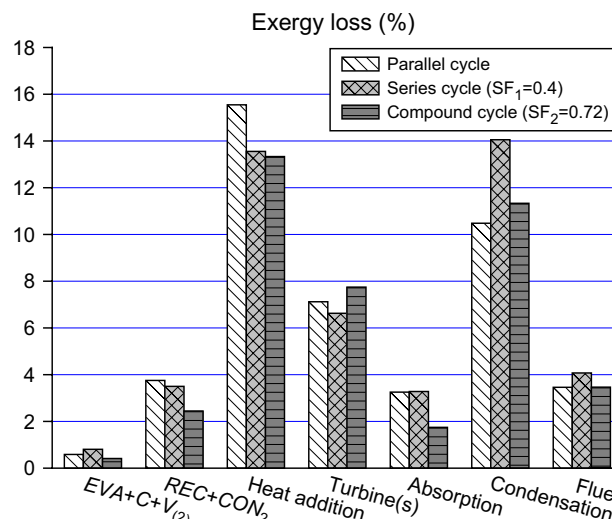Fig. 2. The heat exchange *t*–*Q* diagram in the parallel cogeneration system.

Fig. 3. Exergy losses in the different processes.

addition process is relatively high (15.5%) and in the condensation process is smaller (10.5%).

5. The series-connected cogeneration cycle

Parallel or series connection, here between the refrigeration and power sub-cycles, are the two basic interconnection ways in process engineering and many other fields. Thorough investigation of these two basic ways will thus help us gain a better understanding of more complex configurations and of the methodology for designing more effective systems.

In the parallel system, the working fluid in the refrigeration sub-cycle has the highest concentration, and in the power sub-cycle the lowest. Consequently, the desired temperature glide in the power sub-cycle boiling process does not occur. In the series-connected system proposed in this section, the power sub-cycle is downstream of the refrigeration cycle, thus allowing the use of a relatively strong solution, with a consequent desirable temperature glide, in its heat addition process. At the same time there are also some impairments: the working fluid is brought into the power cycle at a lower temperature and pressure than in the parallel cycle, and the turbine back-pressure is relatively higher because of the relatively high working fluid concentration.

The cycle layout is shown in Fig. 4. The refrigeration cycle can be identified as 15–16–17–18–19, followed by the power cycle: 20–21–22–23–24. 1–2–3–4–5/13–···–7/15 is the preheat and rectification process. The weak solution from the reboiler is split into two streams in the splitter SP: one stream (10) merges with stream 19 to accomplish the absorption process in the high pressure absorber ABS_H and form the turbine working fluid with the intermediate concentration; and the remainder (11) is sent to the power sub-cycle and mixes with the turbine exhaust in the low pressure absorber
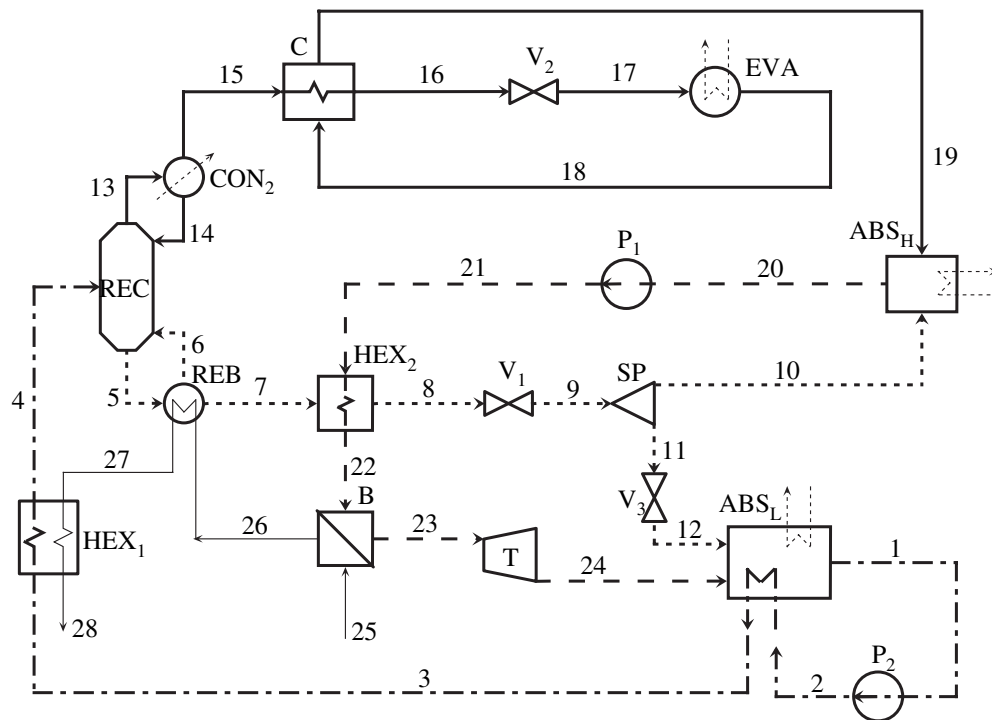
Fig. 4. The flow sheet of the series-connected power/refrigeration cycle. ABS, absorber; B, boiler; C, cooler; CON, condenser; EVA, evaporator; HEX, heat exchanger; P, pump; REB, reboiler; REC, rectifier; SP, splitter; T, turbine; V, valve. (———) high concentration (refrigeration sub-cycle); (– – – –) intermediate concentration (power sub-cycle); (–·—·—) basic concentration; (········) low concentration; (———) heat source fluid; (···········) cooling water.

ABS_L. This has two advantages: (1) the working fluid concentration in the power cycle boiling process can be adjusted to match the variable temperature heat source fluid, and (2) the turbine exhaust fluid is diluted in the low pressure absorber ABS_L by a part of the weak solution (12), bringing its concentration back to the basic value (1), thus reducing the condensation pressure somewhat and increasing the turbine power output.

The heating fluid follows the path of 25–26–27–28. Table 4 summarizes the stream parameters of the flow sheet in Fig. 4, the calculation was based on 1 kg/s basic working fluid feed to the rectifier. The computed cycle performance is reported in Table 5 (the right column).

The SP split fraction SF_1 ($=m_{11}/m_9$) is a key parameter to the cycle performance. When the split fraction is 0, the low pressure absorber ABS_L is eliminated, replaced by a common condenser. Then in the power sub-cycle, the working fluid concentration is the same basic value in both the heat addition process in the boiler and the condensation process. As the split fraction increases, more of the dilute working fluid bypasses the high pressure absorber and the turbine and is sent to the low pressure absorber (ABS_L) directly. On one hand, this raises the concentration of turbine working fluid, but on the other hand, the turbine inlet working fluid mass flow rate decreases, and leads to less power generation, but the boiler B heat demand decreases too. For the purpose

of comparison, calculations are also made for the case of $SF_1 = 0$, and results are reported in Table 5 too.

Table 5 shows that the working fluid concentration in the power cycle heat addition process (21–22–23) increases from 0.25 to 0.324 when SF_1 increases from 0.0 to 0.4, at the same time the mass flow rate for power generation drops from 1.0 to 0.67 kg/s. The refrigeration capacity remains the same, the power output decreases by more than 30%, and the demand for external heat decreases too by 34%. Further analysis suggests that there exist values of SF_1, which maximize the thermal or exergy efficiencies.

When SF_1 is varied in a large range, the refrigeration capacity remains unchanged but the power output and the refrigeration/power ratio R will vary too.

Fig. 5 is the t–Q diagram of the cycle heat addition process for $SF_1 = 0.4$, and the turbine inlet pressure chosen (15,300 kPa) was the one that gave the highest exergy efficiency, which is much higher than the one we have for the parallel cycle, and requires a special high pressure design of boiler, turbine and HEX_2. The amount of heat needed in the evaporation process is only a small portion of the total heat demand, leading to a better thermal match in the boiler heat transfer process.

The efficiencies are somewhat lower than those of the parallel cycle despite the higher turbine inlet pressure. The turbine back-pressure is determined by the working fluid

Table 4
The cycle stream states for the series-connected cogeneration system (the state numbers refer to Fig. 4)

State no.	t (°C)	p (kPa)	Vapor fraction	h (kJ/kg)	s (kJ/kg K)	m (kg/s)	X
Working fluid							
1	35	82.8	0	−13,095.6	−9.728	1	0.25
2	35.2	1484	0	−13,093.4	−9.725	1	0.25
3	72.3	1463	0	−12,900.5	−9.155	1	0.25
4	128.8	1442	0	−12,524.3	−8.211	1	0.25
5	141.7	1400	0	−13,073.8	−7.83	1.06	0.193
6	165	1400	1	−7564.46	−4.385	0.238	0.522
7	165	1400	0	−14,131.9	−7.537	0.82	0.098
8	54.6	1358	0	−14,698.9	−8.97	0.82	0.098
9	54.8	155	0	−14,698.9	−8.966	0.82	0.098
10	54.8	155	0	−14,698.9	−8.966	0.492	0.098
11	54.8	155	0	−14,698.9	−8.966	0.328	0.098
12	54.8	85.3	0	−14,698.9	−8.966	0.328	0.098
13	105.6	1400	1	−3129.75	−6.352	0.234	0.945
14	39	1400	0	−4519.94	−10.649	0.054	0.945
15	39	1400	0	−4519.94	−10.649	0.18	0.945
16	−10	1358	0	−4798.71	−11.622	0.18	0.945
17	−21.6	165	0.046	−4798.74	−11.555	0.18	0.945
18	−15	160	0.738	−3842.35	−7.764	0.18	0.945
19	7.8	155	0.888	−3563.58	−6.693	0.18	0.945
20	36.2	150	0	−12,234.8	−9.906	0.672	0.324
21	39.3	15,708	0	−12,209.2	−9.859	0.672	0.324
22	132.3	15,479	0	−11,516.9	−8.074	0.672	0.324
23	450	15,250	1	−9250.99	−3.973	0.672	0.324
24	83.6	85.3	0.88	−10,115.8	−3.61	0.672	0.324

No.	t (°C)	p (kPa)	Vapor fraction	h (kJ/kg)	s (kJ/kg K)	m (kg/s)	Mole composition	
							N_2	O_2
Heat source fluid								
25	465	104.3	1	459.725	1.081	6.04	0.79	0.21
26	228	103.3	1	207.497	0.673	6.04	0.79	0.21
27	156.7	102.3	1	133.957	0.517	6.04	0.79	0.21
28	95.7	101.3	1	71.628	0.364	6.04	0.79	0.21

condensation temperature in the low pressure absorber ABS_L. The variation of SF_1 has no effect on the turbine back-pressure. The turbine back-pressure (85.3 kPa) is much higher than that in the previous parallel cogeneration system. The exergy analysis results (Fig. 3) indicate that: compared with the parallel configuration, the series one has less exergy loss in the heat addition process by 2% points, but has 3.6% points more exergy loss in the condensation process.

6. The compound cogeneration cycle

In the above discussed parallel system, the working fluid in the power sub-cycle has a fairly low concentration, so it is hard to achieve the best temperature glide and consequent thermal match in the boiling process with the heating fluid, but, on the other hand, the turbine may have a desirable low back-pressure. The opposite happens in the series-connected

cycle: the working fluid has a higher ammonia concentration in the heat addition process and thus a better temperature glide and heat transfer match, but the turbine back-pressure is high, thus reducing power output and increasing the exergy loss in the condensation process. The ideal system should have low exergy losses in both the heat addition and condensation processes. To address an improvement in this direction, we now propose and analyze, a more complex cycle configuration, based on the parallel cogeneration cycle of Section 4. The major difference is the addition of another power route 5—14—15—16 as shown in Fig. 6, to reduce the irreversibility in the cycle heat addition process.

Now the working fluid with the basic ammonia concentration (3) is divided by the splitter SP into two streams (4) and (5). Stream (4) is sent to the rectifier REC, where it is separated into ammonia-rich vapor (19) and ammonia-weak solution (6). The weak solution is further weakened to state (8) in the reboiler by boiling off ammonia-rich vapor

Table 5
Cycle performance summary for the series-connected cogeneration system

Split fraction SF_1	0.0	0.4
Basic solution concentration	0.25	0.25
Intermediate solution concentration	0.25	0.324
Turbine working fluid mass flow rate (kg/s)	1.0	0.672
Turbine inlet temperature (°C)	450	450
Turbine inlet pressure (kPa)	11,700	15,250
Turbine back-pressure (kPa)	85.3	85.3
Minimum heat transfer temperature difference in heat addition process (°C)	15	15
Turbine power output (kW)	844.76	581.04
Pump work (kW)		
P_1	2.2	2.2
P_2	19.1	17.2
Cycle input (kW)		
Reboiler	443.87	443.87
Boiler	2542.98	1522.4
Heat exchanger HEX_1	350.87	376.2
Cycle output (kW)		
Cooling capacity Q_{EVA}	171.82	171.82
Net power output W	823.46	561.6
Refrigeration/power ratio R	0.209	0.306
Heat source fluid		
Mass flow rate (kg/s)	9.17	6.04
Inlet temperature (°C)	465.0	465.0
Energy input Q_{in} (kW)	4217.13	2776.24
Exergy input E_{in} (kW)	1664.16	1095.55
Thermal efficiency η_1 (%)	23.60	26.42
Exergy efficiency η_2 (%)	51.36	54.12

(7), and then is sent to the boiler B and turbine T_1, for power generation. The other (stream (5)) is directly brought into one power cycle by being pumped and heated, and then expands in the second turbine T_2, so it is possible to have
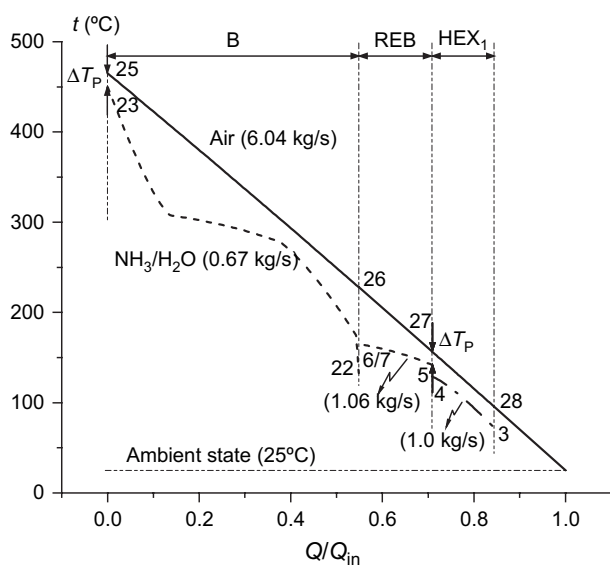

Fig. 5. The heat exchange t–Q diagram in the series-connected cogeneration system ($SF_1 = 0.4$).

a stronger solution at least in this power cycle heat addition process.

There are two power routes in this system: 8–9–10–11–12–13 and 5–14–15–16. The ammonia concentrations of the two turbine working fluids are also different. One is low concentration in 8–9–10–11–12–13 for turbine T_1, the other is the basic concentration in 5–14–15–16 for turbine T_2. The exhausts of the two turbines merge in the low pressure absorber ABS_L to form an intermediate concentration solution (17). In that way the stream (16) is diluted and therefore turbine T_2 may have a lower back-pressure. This compound cycle adopts the Kalina cycle concept of varying working fluid concentration to reduce the turbine back-pressure. The working fluid (8) in the first power route is not only used for power generation, but also as the absorbent in the low pressure absorber, therefore, the condensation process for the second power route is eliminated and replaced with an absorption process.

The cycle performance is calculated and the results are reported in Tables 6 and 7; the calculation was based on a 1 kg/s basic working fluid feed to the splitter SP.

In addition to the advantages of the absorption–condensation, it is found that the heat transfer process in the boiler is improved too. Fig. 7 shows the t–Q diagram of the heat addition process. The two cold streams in the
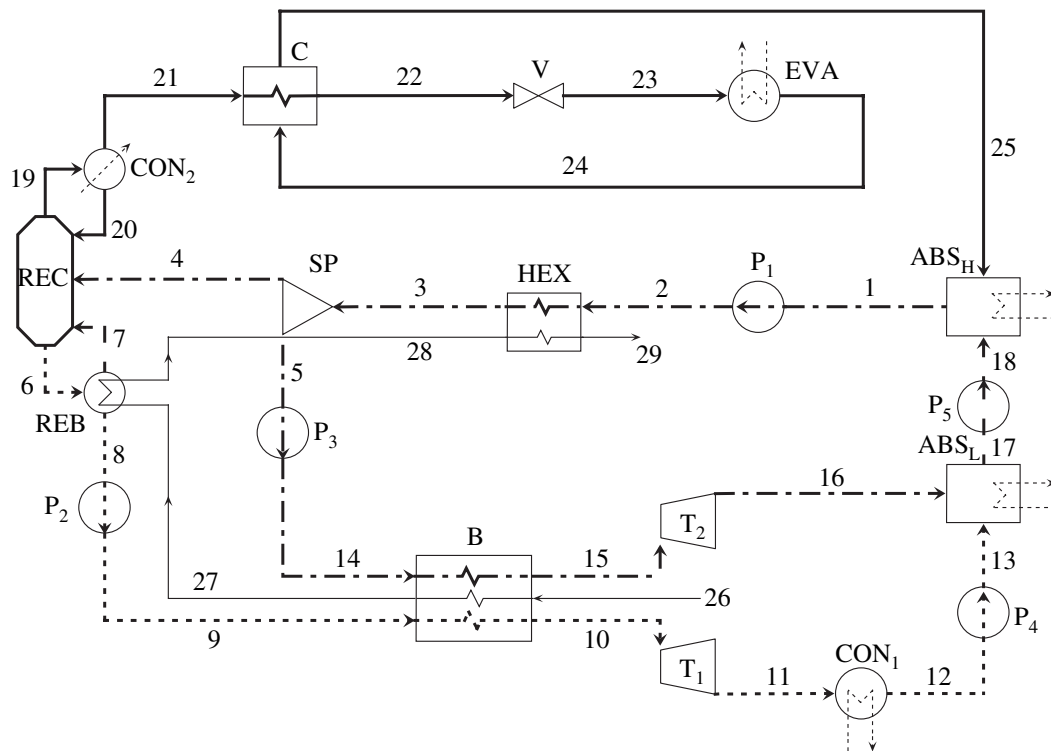
Fig. 6. The flow sheet of the compound power/refrigeration cycle. ABS, absorber; B, boiler; C, cooler; CON, condenser; EVA, evaporator; HEX, heat exchanger; P, pump; REB, reboiler; REC, rectifier; SP, splitter; T, turbine; V, valve. (———) high concentration (refrigeration sub-cycle); (— · — · —) basic concentration (power sub-cycle); (· · · · · · ·) low concentration (power sub-cycle); (– – – –) intermediate concentration; (———) heat source fluid; (· · · · · · · · · · ·) cooling water.

boiler have concentrations of 0.3 and 0.098, respectively; they neither have high ammonia concentrations nor high pressures. The thinner dash–dot–dot line shows a temperature curve of a single cold stream with the ammonia mass fraction of 0.3, heated by the same heating fluid. It can be seen that the combination of the two cold streams has a much better temperature match with the heating fluid, thus reducing the irreversibility of the heat transfer process.

An exergy analysis is conducted and the results are reported in Fig. 3 for comparison. Compared with the parallel cycle, the exergy loss in the heat addition process drops by 2.2% points; compared with the series cycle, the exergy loss in the condensation process drops by 2.7% points; all attributed to the improvement of thermal match in both the heat addition and the condensation process. It is noticed that the compound cycle also has the least exergy loss in the (REC + CON$_2$) and the absorption process in ABS$_H$, because the REC and ABS$_H$ only deal with a fraction (72%) of the basic working fluid.

Similar to the series-connected system, the split ratio in the splitter, defined as SF$_2$ = m_4/m_3, is also a key parameter for this cycle. It is easy to see that when SF$_2$ = 1 the cycle becomes the parallel one described in Section 4.

The effects of SF$_2$ on the cycle performance are investigated and the results are shown in Fig. 8. As SF$_2$ increases,

more basic concentration working solution is sent to the rectifier, leading to the increase of the refrigeration output. At the same time, the mass flow rate of working fluid to turbine T$_1$ increases, but to turbine T$_2$ decreases, resulting in an SF$_2$ which maximizes the power output (Fig. 8a).

The concentration of the working fluid of turbine T$_1$, remains at a constant low level in both the boiling process (in B) and the condensation process (in CON$_1$), thus leaving the back-pressure of turbine T$_1$ unchanged, at about 19 kPa. When SF$_2$ varies, however, the concentration of the mixture (state 17) at the two turbine exhausts varies too, which has some effect on the back-pressure of turbine T$_2$. This is because a weaker solution has a lower pressure for the same bubble point temperature; as seen in Fig. 8b, the concentration of stream (17) decreases when SF$_2$ increases, leading to the decrease of the back-pressure of turbine T$_2$.

In this calculation, the inlet pressures for the two turbines are set to be the same, at a value that produces the highest exergy efficiency with the parameters in Table 1 held constant. The two constraints for the optimization are the minimum (pinch point) heat transfer temperature difference in the boiler (15 K) and the minimum turbine exhaust vapor fraction (0.88). The variation of $p_{T,i}$ is shown in Fig. 8c. The mass flow rate of the heating fluid does not change much, and has its lowest value when SF$_2$ ≈ 0.9.

Table 6
The cycle stream states for the compound cogeneration system (the state numbers refer to Fig. 6)

State no.	t (°C)	p (kPa)	Vapor fraction	h (kJ/kg)	s (kJ/kg K)	m (kg/s)	X
Working fluid							
1	40.4	150	0	−12,494.4	−9.775	1	0.3
2	40.7	1484	0	−12,492.2	−9.771	1	0.3
3	117.9	1442	0	−12,030.1	−8.535	1	0.3
4	117.9	1442	0	−12,030.1	−8.535	0.72	0.3
5	117.9	1442	0	−12,030.1	−8.535	0.28	0.3
6	134.5	1400	0	−12,758.7	−7.905	0.783	0.221
7	165	1400	1	−7564.46	−4.385	0.228	0.522
8	165	1400	0	−14,131.8	−7.537	0.555	0.098
9	167	7674	0	−14,119.9	−7.526	0.555	0.098
10	450	7580	1	−11,635.2	−2.986	0.555	0.098
11	56.6	19.1	0.88	−12,610	−2.544	0.555	0.098
12	35	18.6	0	−14,789.8	−9.248	0.555	0.098
13	35	40	0	−14,789.7	−9.248	0.555	0.098
14	119	7670	0	−12,017.7	−8.517	0.28	0.3
15	450	7580	1	−9409.06	−3.459	0.28	0.3
16	66.8	40	0.919	−10,321.9	−3.058	0.28	0.3
17	35	38.8	0	−14,044.5	−9.474	0.835	0.166
18	35	155	0	−14,044.3	−9.474	0.835	0.166
19	88.2	1400	1	−2805.58	−6.628	0.215	0.979
20	37.5	1400	0	−4082.99	−10.696	0.05	0.979
21	37.5	1400	0	−4082.99	−10.696	0.165	0.979
22	−9.2	1358	0	−4341.8	−11.562	0.165	0.979
23	−22.7	165	0.051	−4341.79	−11.524	0.165	0.979
24	−15	160	0.9	−3181.79	−6.893	0.165	0.979
25	32.5	155	0.99	−2922.98	−5.947	0.165	0.979

No.	t (°C)	p (kPa)	Vapor fraction	h (kJ/kg)	s (kJ/kg K)	m (kg/s)	Mole composition	
							N_2	O_2
Heat source fluid								
26	465	104.3	1	459.725	1.081	7.6	0.79	0.21
27	203.4	103.3	1	182.074	0.621	7.6	0.79	0.21
28	149.5	102.3	1	126.586	0.5	7.6	0.79	0.21
29	89.9	101.3	1	65.744	0.348	7.6	0.79	0.21

Fig. 8d shows the variations of the efficiencies. The SF_2 that maximizes the exergy efficiency is about 0.72, and the SF_2 maximizing the energy efficiency is higher. The base-case cycle has very good thermal performance with the energy efficiency and exergy efficiency of 28% and near 60%, respectively, as reported in Table 7. The good thermal match in the boiler is obtained by the arrangement of two cold streams with different low ammonia concentrations, rather than one high concentration cold stream; and the back-pressures of both turbines can be maintained at a lower level because of the low ammonia concentration and the adoption of absorption−condensation. The irreversibility in both the power cycle heat addition process and condensation process can thereby be reduced.

If the cycle main parameters in Table 1 remain constant, the refrigeration capacity and power output in the parallel cycle cannot be adjusted. In the series-connected cycle, only the power output can be adjusted, by varying SF_1. In the compound cycle, the variation of SF_2 has effects on both refrigeration capacity and power output, so the refrigeration/power output ratio R can be easily adjusted by varying the value of SF_2.

We note that the parallel cycle has the highest refrigeration/power ratio R of 0.37, and the compound one has the lowest R of 0.25. For the same heating fluid mass flow rate, the compound cycle can produce 9 and 11% more power and 28 and 11% less refrigeration, respectively, than the parallel and series-connected systems. Its exergy efficiency is 4 and 5% points higher, respectively, than those of the parallel and series-connected systems.

7. Concluding remarks

This paper shows the implementation of some general principles for refrigeration and power cogeneration system integration and design, with ammonia−water mixture as

Table 7
Cycle performance summary for the compound cogeneration system

Split fraction SF_2	0.72
Turbine T work (kW)	
T_1	540.78
T_2	255.61
Pump work (kW)	
P_1	2.18
P_2	6.74
P_3	3.56
P_4	0.017
P_5	0.15
Refrigeration output Q_{EVA} (kW)	191.66
Condenser CON_1 load (kW)	1209.28
Rectifier condenser CON_2 load (kW)	274.37
Cooler C load (kW)	42.75
Absorber heat load (kW)	
ABS_H	628.85
ABS_L	287.6
Boiler B heat input (kW)	2108.64
Reboiler REB heat input (kW)	421.43
Heat exchanger HEX heat input (kW)	462.12
Net power output W (kW)	783.75
Refrigeration/power ratio R	0.245
Heat input Q_{in} (kW)	3493.26
Exergy input E_{in} (kW)	1378.51
Energy efficiency η_1 (%)	27.92
Exergy efficiency η_2 (%)	59.5

the working fluid. The well-known principles, and the way they were implemented in this development, are:

(1) both the external heat input and heat exchanged within the cycle components should be used/recovered properly and thoroughly: an important way for that is to cascade the heat exchange according to the temperature of both hot and cold streams.

This principle was followed here by creating a component configuration cascaded, heat source to sink, by their temperatures. To generate more power, the turbine working fluid needs to be heated to as high a temperature as possible in the boiler. The reboiler at the bottom of the rectifier needs mid-temperature heat to boil off the ammonia-rich vapor. Therefore, to match with the heating fluid, the boiler was placed at the highest temperature region, followed by the reboiler. Lower in the cascade, the heating fluid at the outlet of the reboiler was used to preheat the working fluid feed to the rectifier, helping to reduce the reboiler load.

(2) To obtain a good temperature match with the sensible heat source, the working fluid must exhibit an appropriate temperature glide in the boiler, that was accomplished here by ensuring that its concentration in the evaporation process is neither too high nor too low.

(3) Higher back-pressure helps prevent air leakage into the system, but reduces the turbine power output.

To examine the potential to increase cycle efficiency, in this paper, the turbine is set to expand to the lowest possible back-pressure to generate more power output and to reduce the exergy loss in the condensation process.

Principles 2 and 3 are not always easy to satisfy at the same time in the ammonia—water system, and a splitting and absorption unit are therefore employed to adjust some stream mass flow rates and thus maintain the desired ammonia concentrations in both the heat addition process and the absorption process, in the series-connected and the compound cogeneration systems. That unit brings a stronger solution into the power sub-cycle heat addition process, thus making a better temperature match with the heating fluid. It also dilutes at the same time the turbine exhaust in the absorption—condensation process, leading to a drop of the turbine back-pressure and improvement of the temperature match in the condensation process.

(4) The exergy loss associated with pressure drops needed for the process should be minimized, for example by substituting a throttling process with a power generation one, as accomplished in the parallel and compound systems.

In the three cycle configurations analyzed, the energy and exergy efficiencies were found to be 26—28% and 55—60%, respectively, in the base-case when the top heat input temperature is 450 °C. That efficiency is, by itself, excellent for cycles using heat sources of ~450 °C, and the exergy efficiency is comparable to that of nuclear power plants. When using the exhaust heat from topping gas turbine power plants, which, if
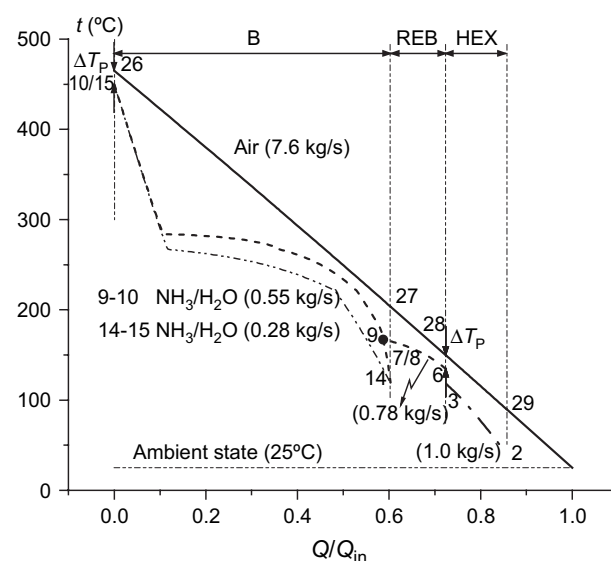

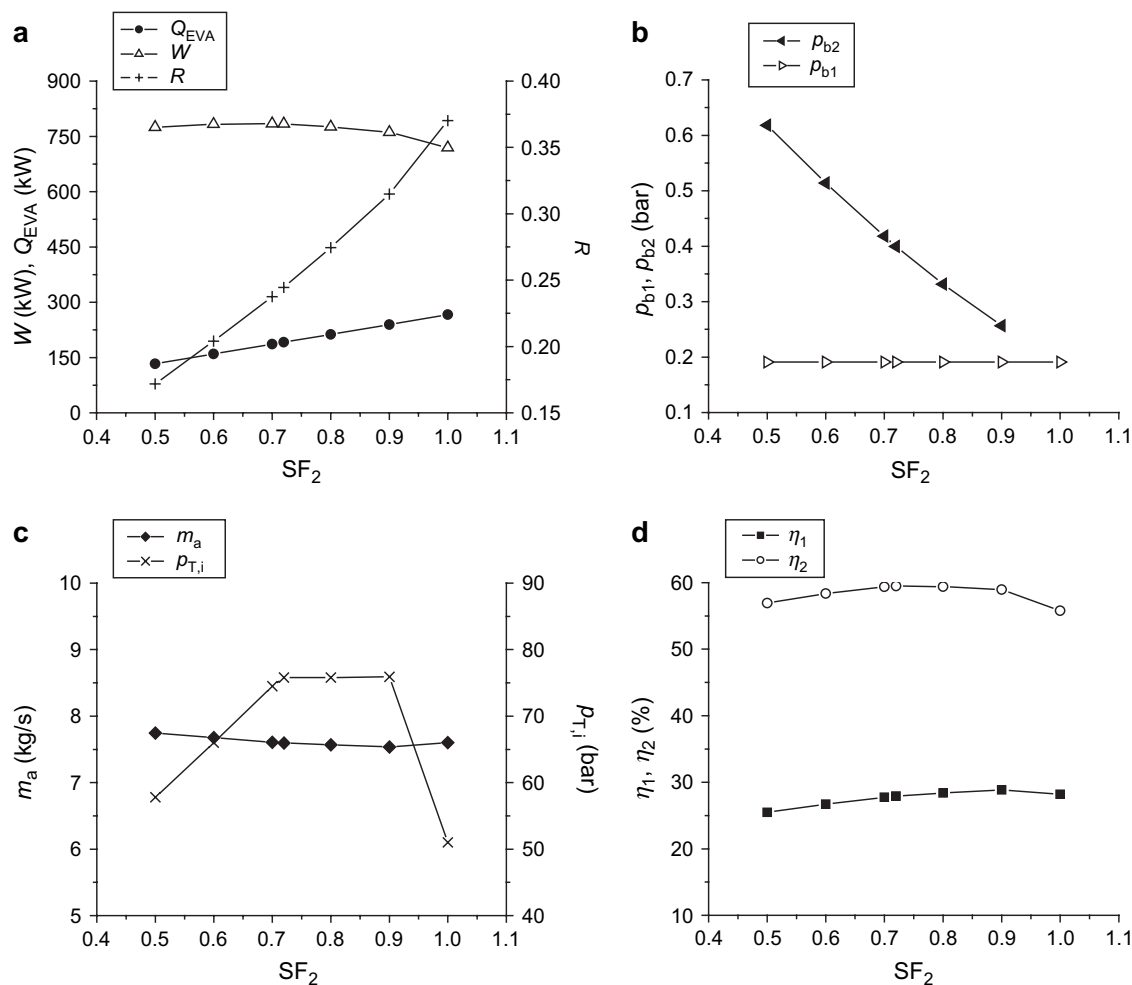Fig. 7. The heat exchange t—Q diagram in the compound cogeneration system ($SF_2 = 0.72$).

Fig. 8. Effect of the split ratio SF_2 on the compound cycle performance. (a) power output, refrigeration capacity and the refrigeration/power ratio; (b) turbine back-pressures; (c) heating fluid mass flow rate and turbine inlet pressure; (d) energy efficiency and exergy efficiency.

used independently, typically have efficiencies of about 40%, the total plant energy efficiency rises to the remarkable value of about 57%. The hardware used is conventional and commercially available; no hardware additional to that needed in conventional power and absorption cycles is needed.

It is of course of interest to compare the performance and capital investment of the proposed cogeneration system with separate conventional steam Rankine power cycles and absorption refrigeration cycles that produce the same power and refrigeration outputs. Such comparison was made by the authors [18], where it was demonstrated that a somewhat similar cogeneration system operates at better efficiency than the separate cycles, with no penalty in capital equipment.

References

[1] J.H. Horlock, Cogeneration-Combined Heat and Power (CHP) − Thermodynamics and Fluid Mechanics Series, Pergamon, Oxford, 1987.

[2] D.Y. Goswami, Solar thermal technology: present status and ideas for the future, Energy Sources 20 (1998) 137−145.

[3] D.Y. Goswami, F. Xu, Analysis of a new thermodynamic cycle for combined power and cooling using low and mid temperature solar collectors, Journal of Solar Energy Engineering 121 (1999) 91−97.

[4] A.A. Hasan, D.Y. Goswami, Exergy analysis of a combined power and refrigeration thermodynamic cycle driven by a solar heat source, ASME Journal of Solar Energy Engineering 125 (2003) 55−60.

[5] S. Lu, D.Y. Goswami, Optimization of a novel combined power/refrigeration thermodynamic cycle, ASME Journal of Solar Energy Engineering 125 (2003) 212−217.

[6] G. Tamm, D.Y. Goswami, S. Lu, A.A. Hasan, Novel combined power and cooling thermodynamic cycle for low temperature heat sources. Part 1: Theoretical investigation, Journal of Solar Energy Engineering 125 (2003) 218−222.

[7] G. Tamm, D.Y. Goswami, Novel combined power and cooling thermodynamic cycle for low temperature heat sources. Part 2: Experimental investigation, Journal of Solar Energy Engineering 125 (2003) 223—229.

[8] S. Vijayaraghavan, D.Y. Goswami, On evaluating efficiency of a combined power and cooling cycle, ASME Journal of Energy Resources Technology 125 (2003) 221—227.

[9] J.H. Horlock, Advanced Gas Turbine Cycles, Pergamon, Oxford, 2003.

[10] J.D. Maloney, R.C. Robertson, Thermodynamic Study of Ammonia—Water Heat Power Cycles, ORNL Report CF-53-8-43, Oak Ridge, TN, 1953.

[11] A.I. Kalina, Combined-cycle system with novel bottoming cycle, ASME Journal of Engineering for Gas Turbines and Power 106 (1984) 737—742.

[12] O.M. Ibrahim, S.A. Klein, Absorption power cycles, Energy 21 (1) (1996) 21—27.

[13] Y. Wang, W. Han, H. Jin, D. Zheng, A novel binary cycle with mid and low temperature heat recovery, Proceedings of the Chinese Society for Electrical Engineering 23 (2003) 200—204 (In Chinese with English abstract).

[14] L. Gao, Y. Wang, H. Jin, Z. Liu, R. Cai, A novel binary cycle with integration of low-level waste heat recovery & LNG cold energy utilization, Journal of Engineering Thermophysics 23 (2002) 397—400 (In Chinese with English abstract).

[15] N. Lior, N. Zhang, Energy, exergy, and second law performance criteria, Proceedings of ECOS 2005 1 (June 20—22) (2005) 437—445 Trondheim, Norway (expanded version published in Energy 32 (2007) 281—296).

[16] Aspen Plus®, Aspen Technology, Inc., version 11.1. Available from: http://www.aspentech.com/.

[17] International Institute of Refrigeration, Thermodynamic and Physical Properties NH_3—H_2O, Paris, France, 1994.

[18] N. Zhang, R. Cai, N. Lior, A Novel Ammonia—Water Cycle For Power And Refrigeration Cogeneration, ASME paper IMECE2004-60692, Anaheim, CA, American Society of Mechanical Engineers, NY, 2004.